Wah Chiu
wah@bcm.tmc.edu
October 11, 2004

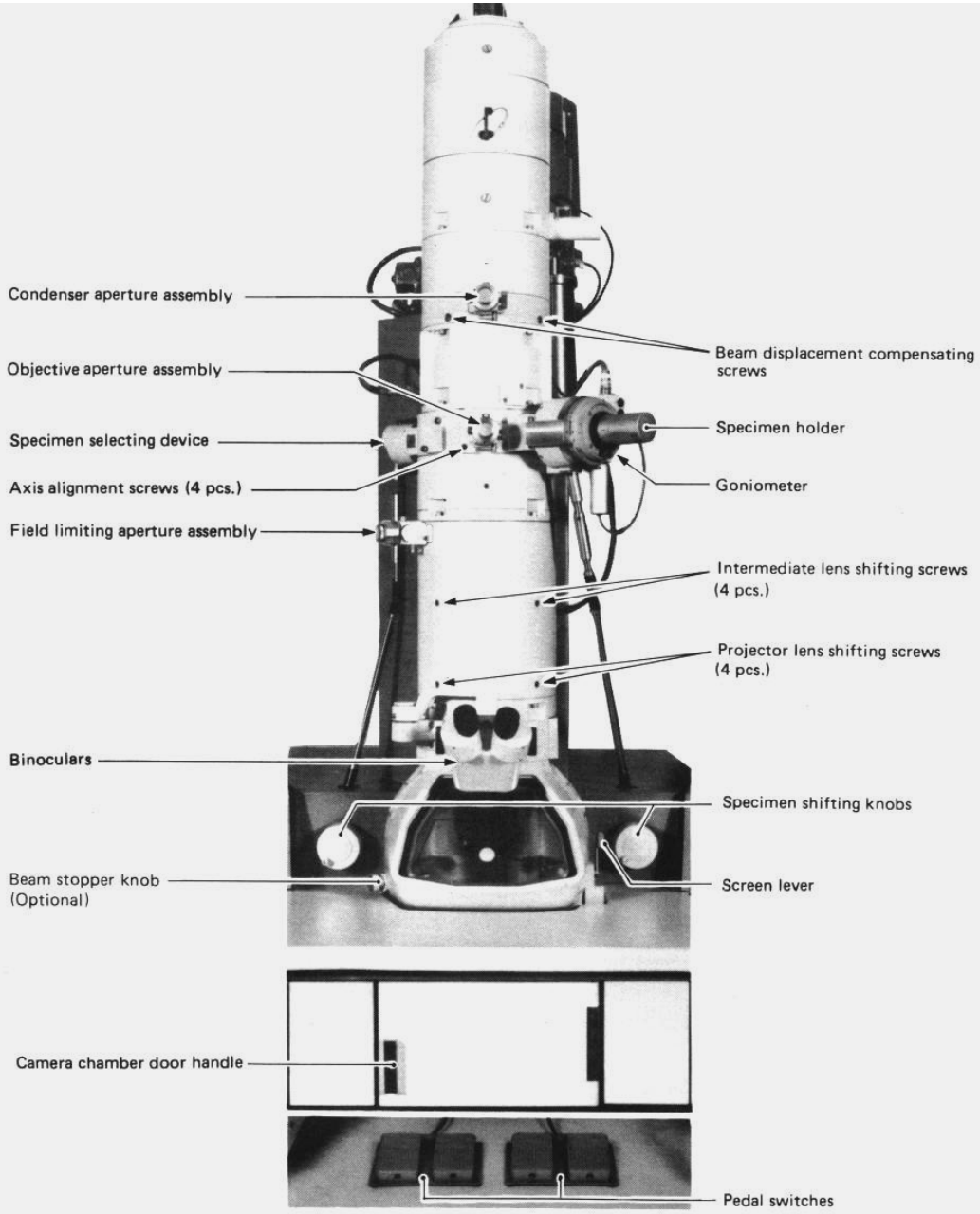

* Optional attachments are included in this photograph.

Fig. 3.3-1 External view of column

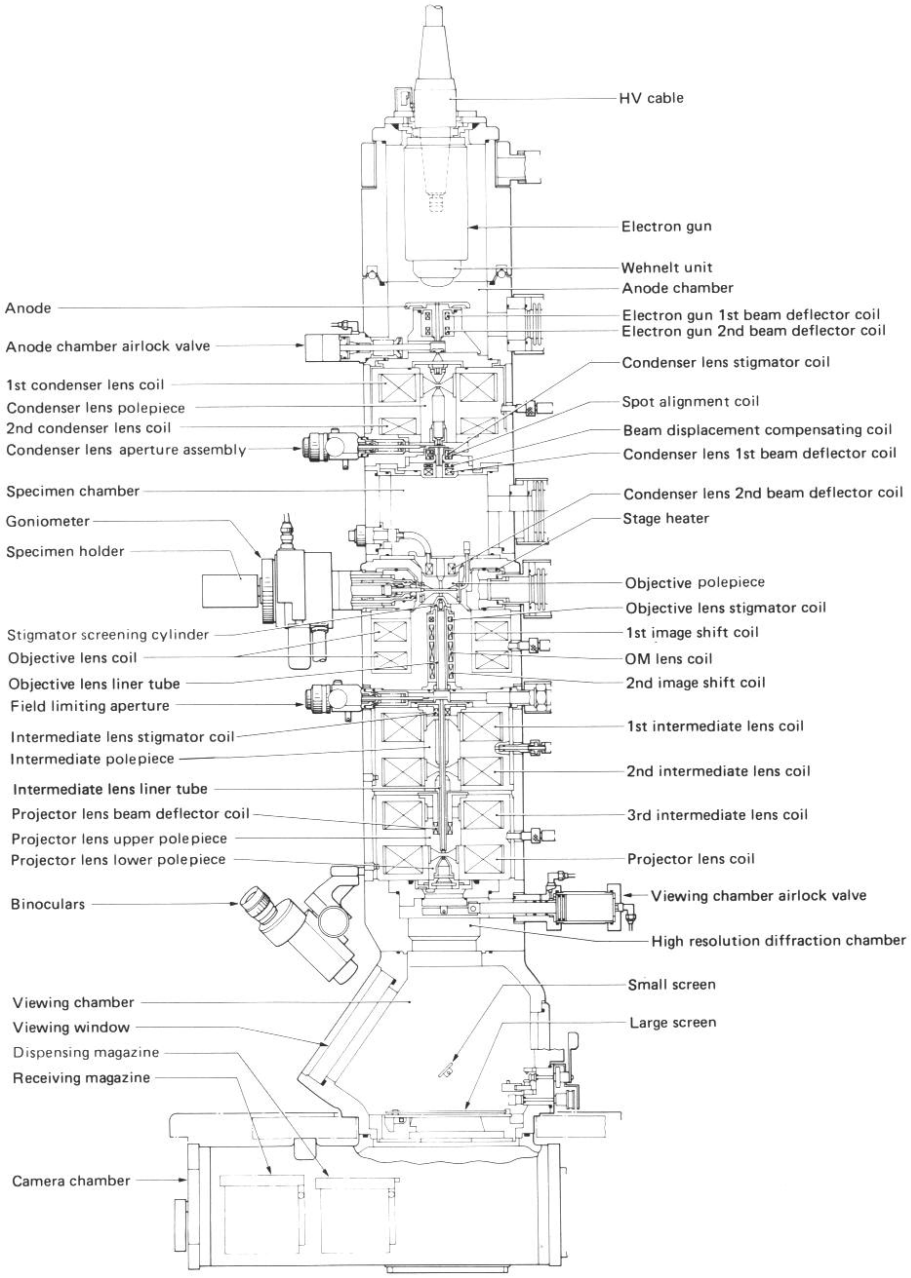

Fig. 3.3-2 Cross section of microscope column

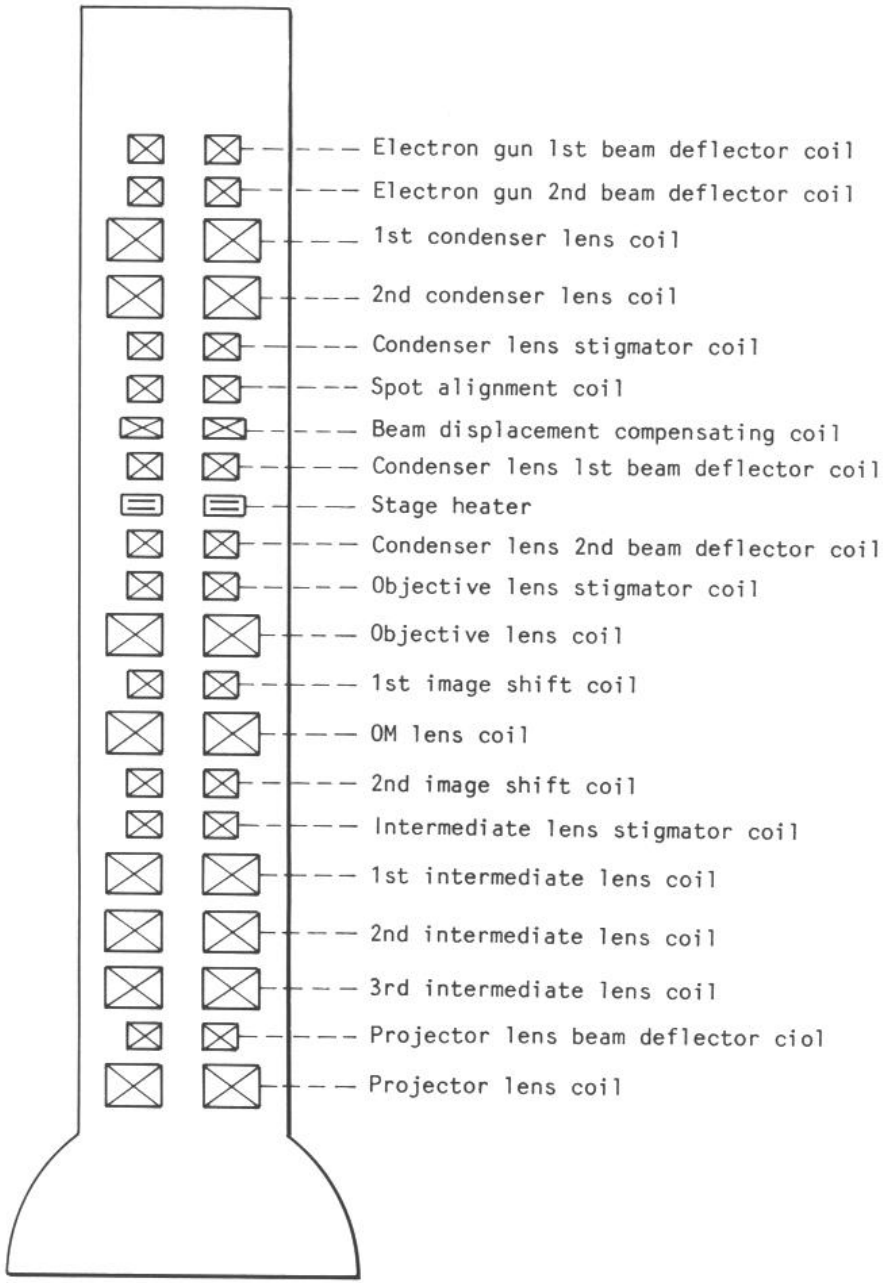

Fig. 3.3-3 Location of lenses and coils

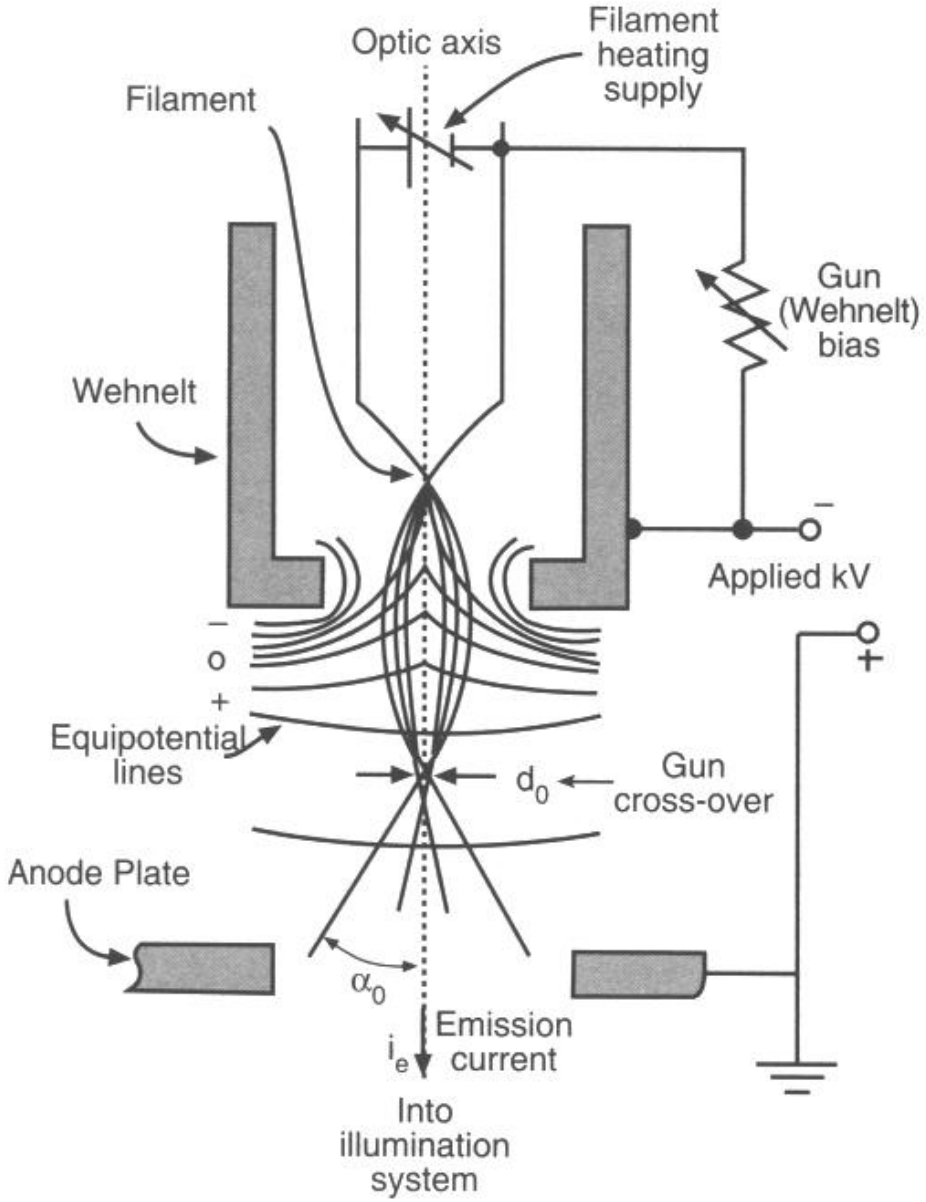

Figure 5.1. Schematic diagram of a thermionic electron gun. A high voltage is placed between the filament and the anode, modified by a potential on the Wehnelt which acts to focus the electrons into a crossover, with diameter d_0 and convergence/divergence angle α_0.

Figure 5.2. The three major parts of a thermionic gun, from top to bottom: the cathode, the Wehnelt cylinder, and the anode, shown separated. The Wehnelt screws onto the cathode (filament) support and both are attached to the high-tension cable which contains power supplies for heating the filament and biasing the Wehnelt. The anode sits just below the Wehnelt, in the top of the TEM column.

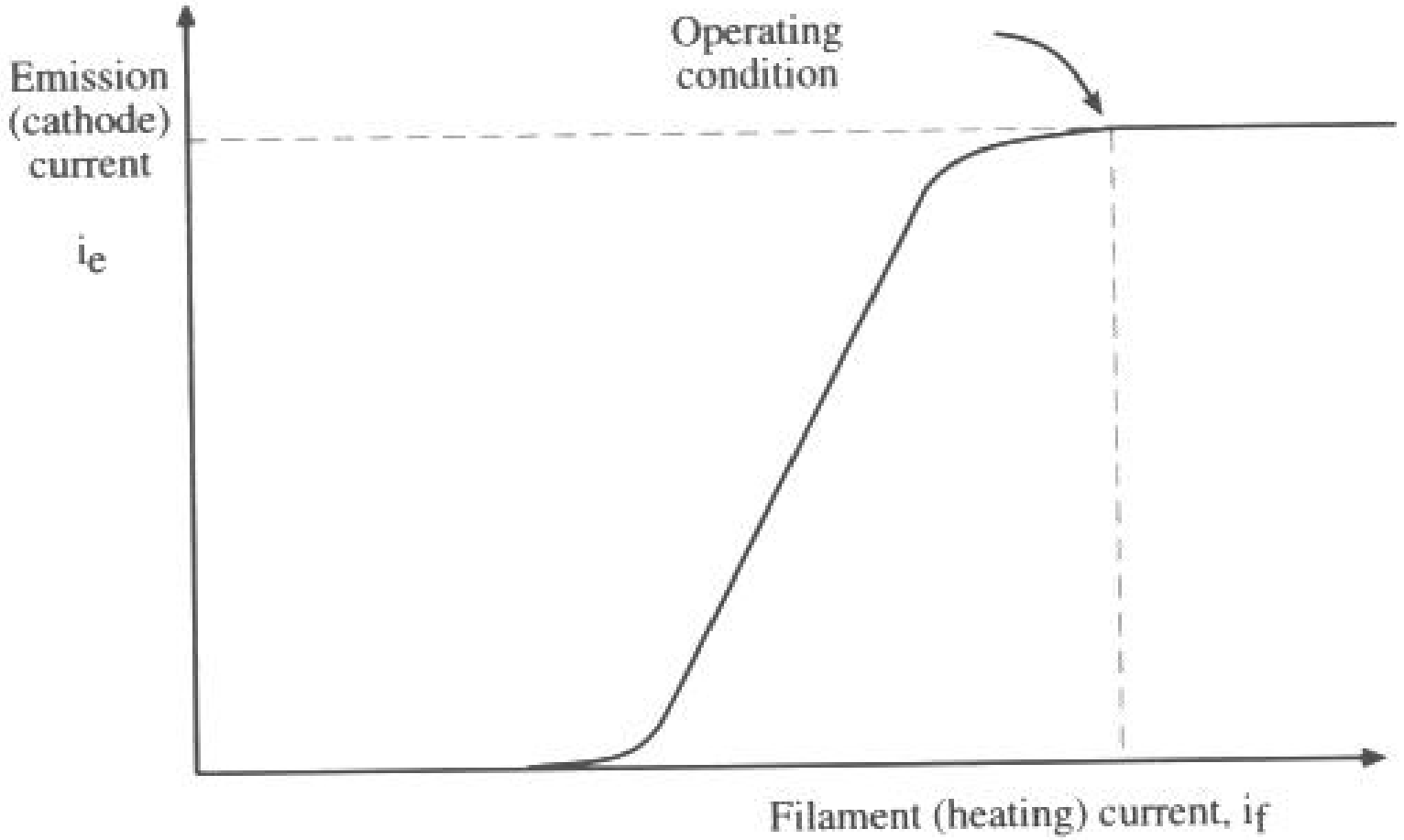

Figure 5.3. The relationship between the current emitted by the electron source (i_e) and the filament heating current (i_f) for a self-biasing gun. Increasing the filament current results in a maximum emission current termed saturation.

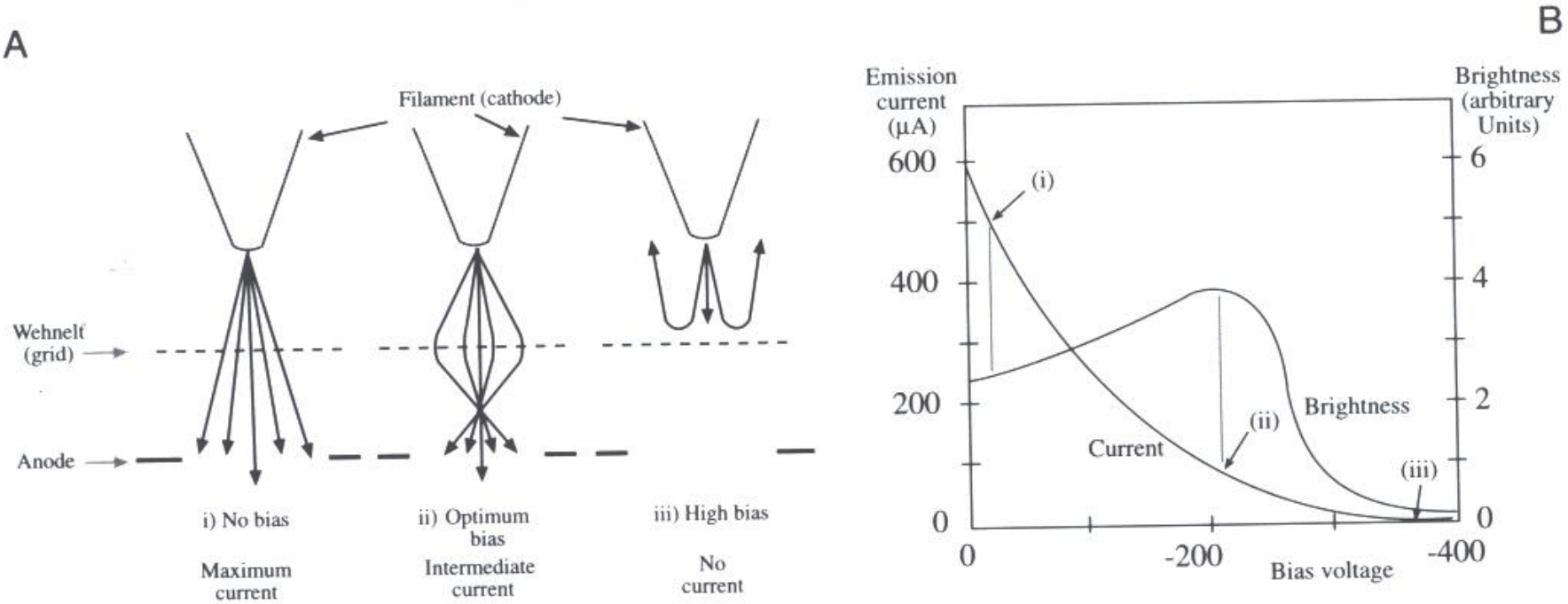

Figure 5.4. (A) The effect of increasing Wehnelt bias (i–iii) on the distribution of electrons coming through the anode. (B) The relationship between the bias and the emission current/gun brightness. Maximum brightness is achieved at an intermediate Wehnelt bias, and an intermediate emission current [condition (ii) in A].

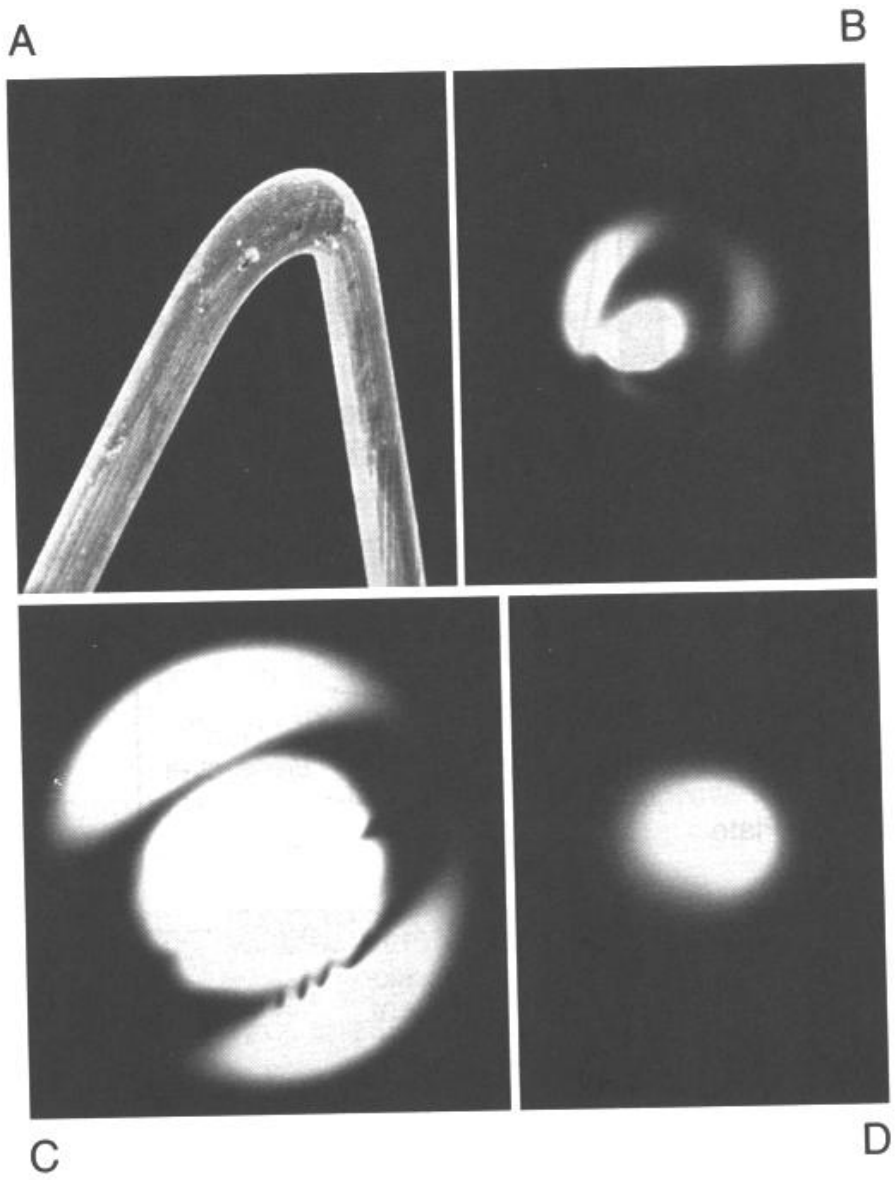

Figure 5.5. (A) The tip of a tungsten hairpin filament and the distribution of electrons when the filament is (B) undersaturated and misaligned, (C) undersaturated and aligned, and (D) saturated.

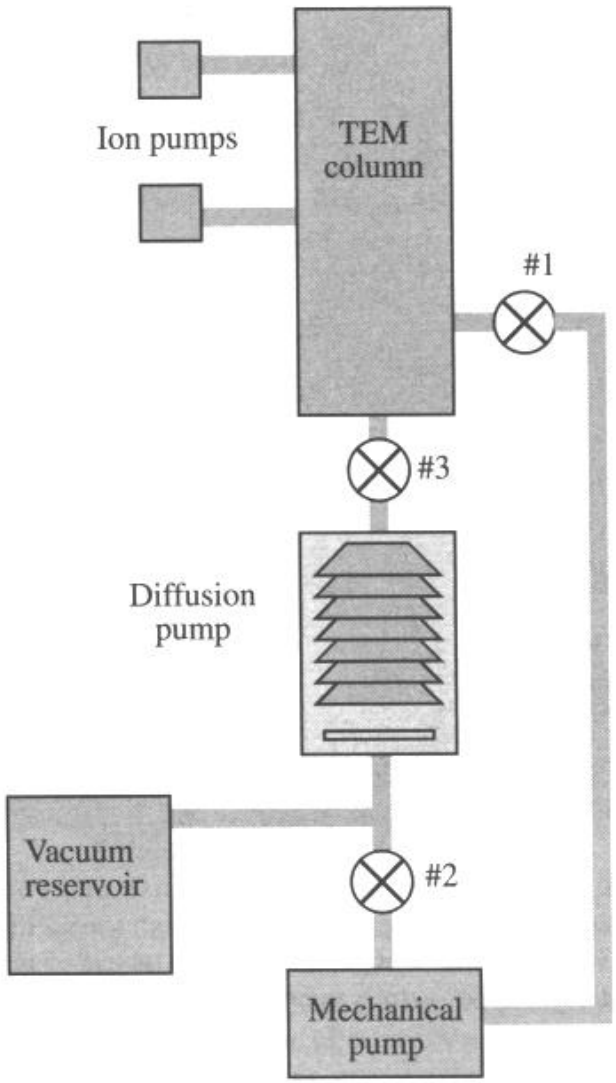

Figure 8.5. The principles of the TEM vacuum system. Often, the console display on the TEM will show a similar diagram. The mechanical pump can pump the column directly or back out the diffusion pump, which is connected directly to the base of the microscope. Ion pumps are often interfaced directly to the stage and gun areas. Computer-controlled valves separate the pumps from the column and from each other.

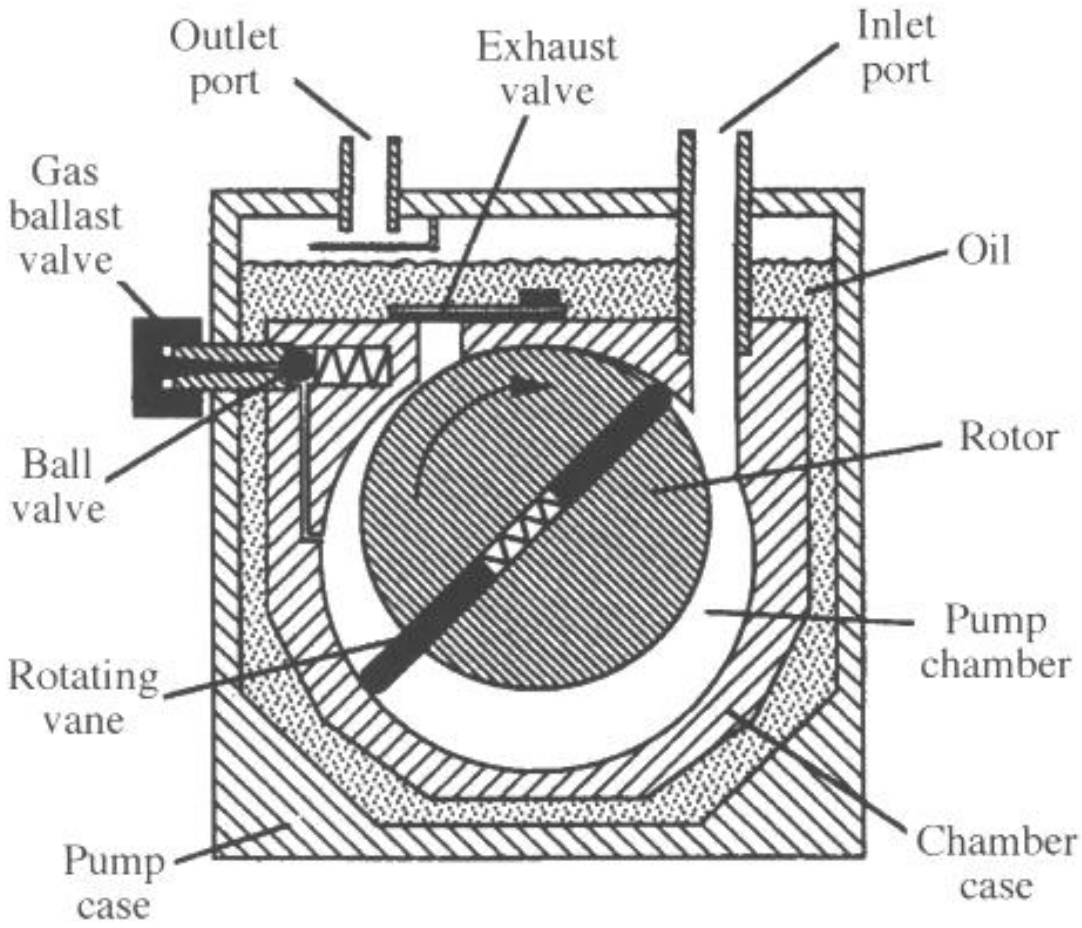

Figure 8.1. A mechanical pump for roughing vacuums. The eccentric motion of the pump creates a vacuum in the RH side when it rotates and the vacuum sucks air into the inlet valve. As the cylinder rotates further, it cuts off the inlet and forces the air through the outlet on the LH side, creating a vacuum again on the inlet side as it does so. Because of the constant contact between the rotating cylinder and the inside of the pump, oil is needed to reduce frictional heating.

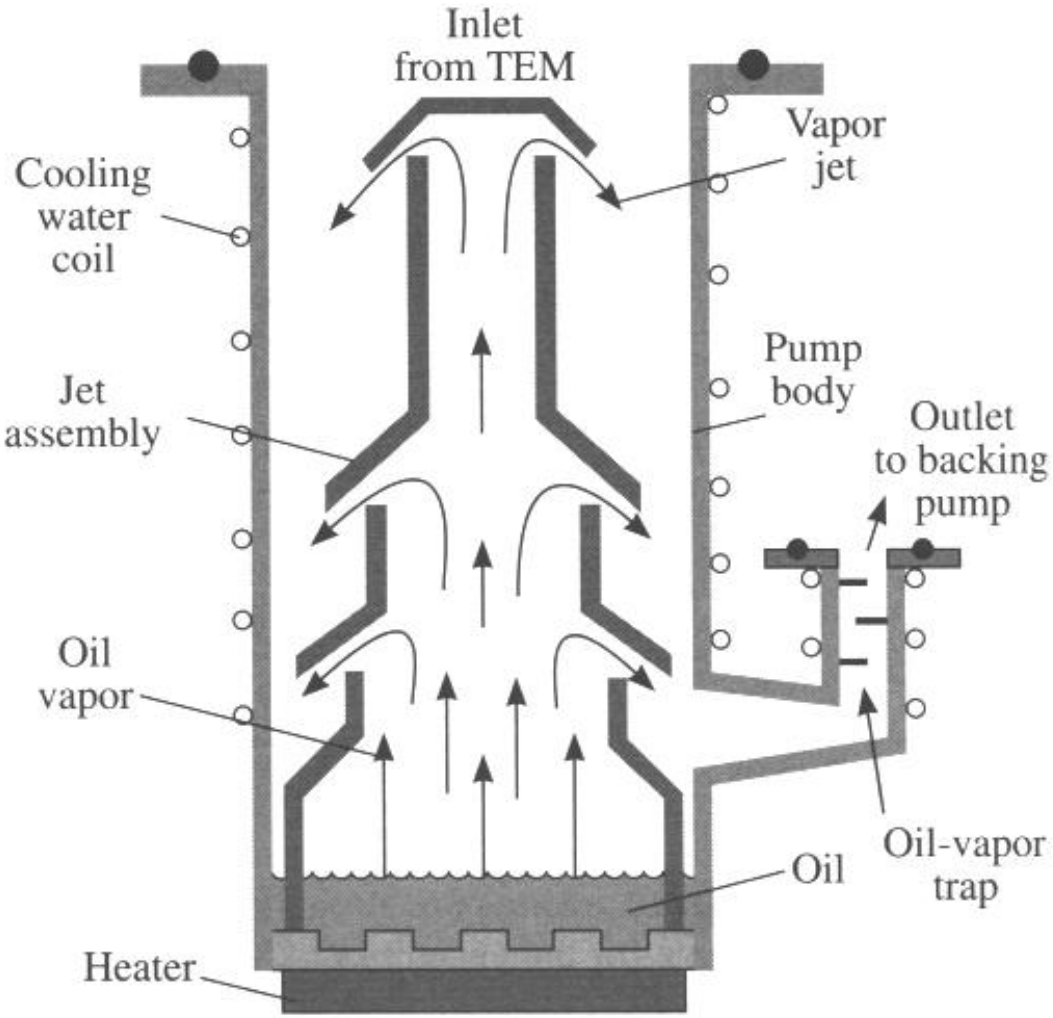

Figure 8.2. Principles of diffusion pump operation. A heater plate at the base of the pump boils synthetic oil. The expansion of the oil vapor on boiling creates a pressure, which forces the vapor up the central column and out of several holes. The stream of oil vapor pulls gas molecules out of the top of the pump down to the base, where the oil condenses and the air is pumped out of the base by a mechanical backing pump.

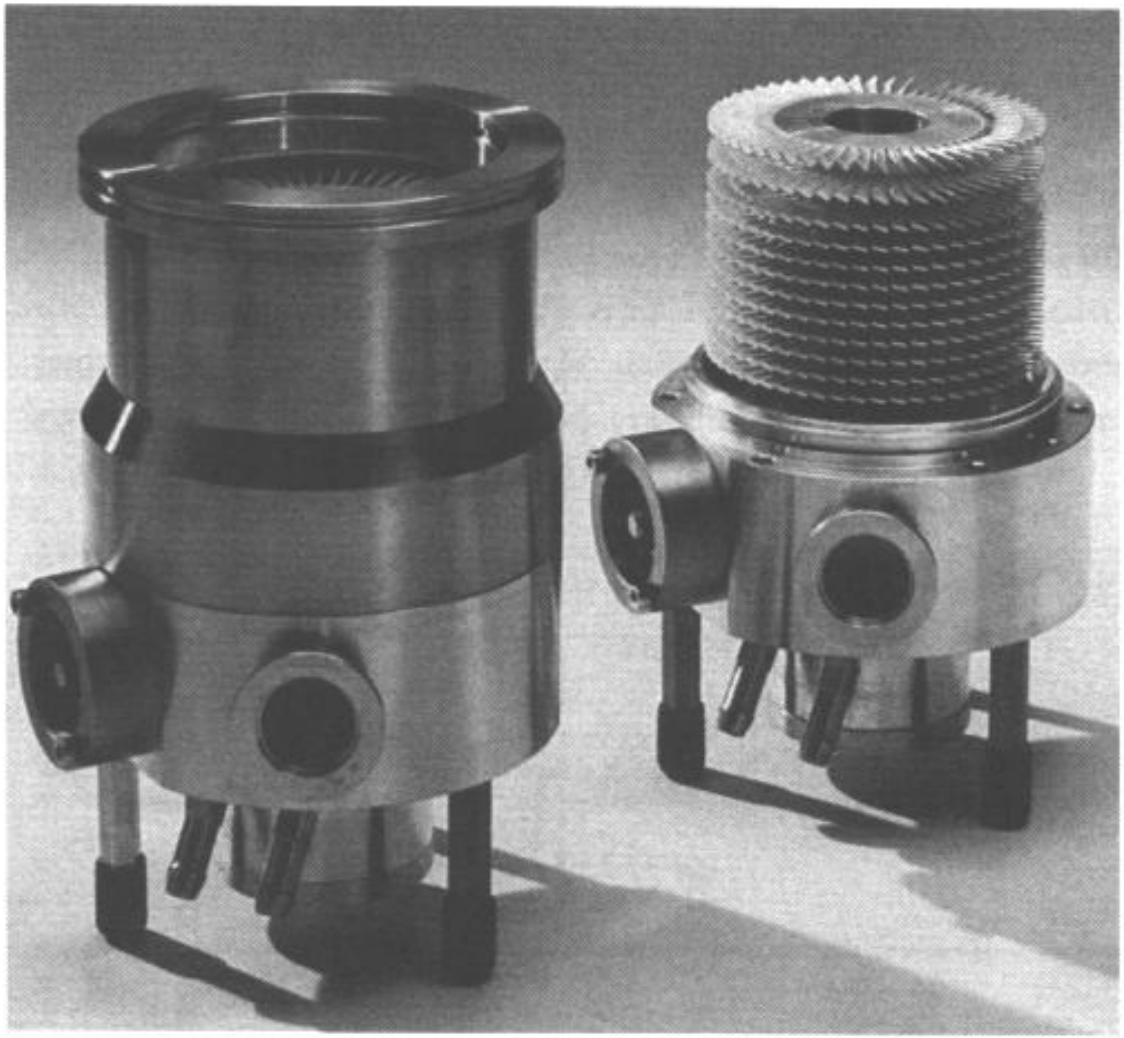

Figure 8.3. A turbopump (with and without its casing) which is nothing more than a small turbine that rotates at high speed. Like a jet turbine it pulls air in at the front end and forces it out of the back. The blades are designed like airfoils to enhance the flow of gas through the system.

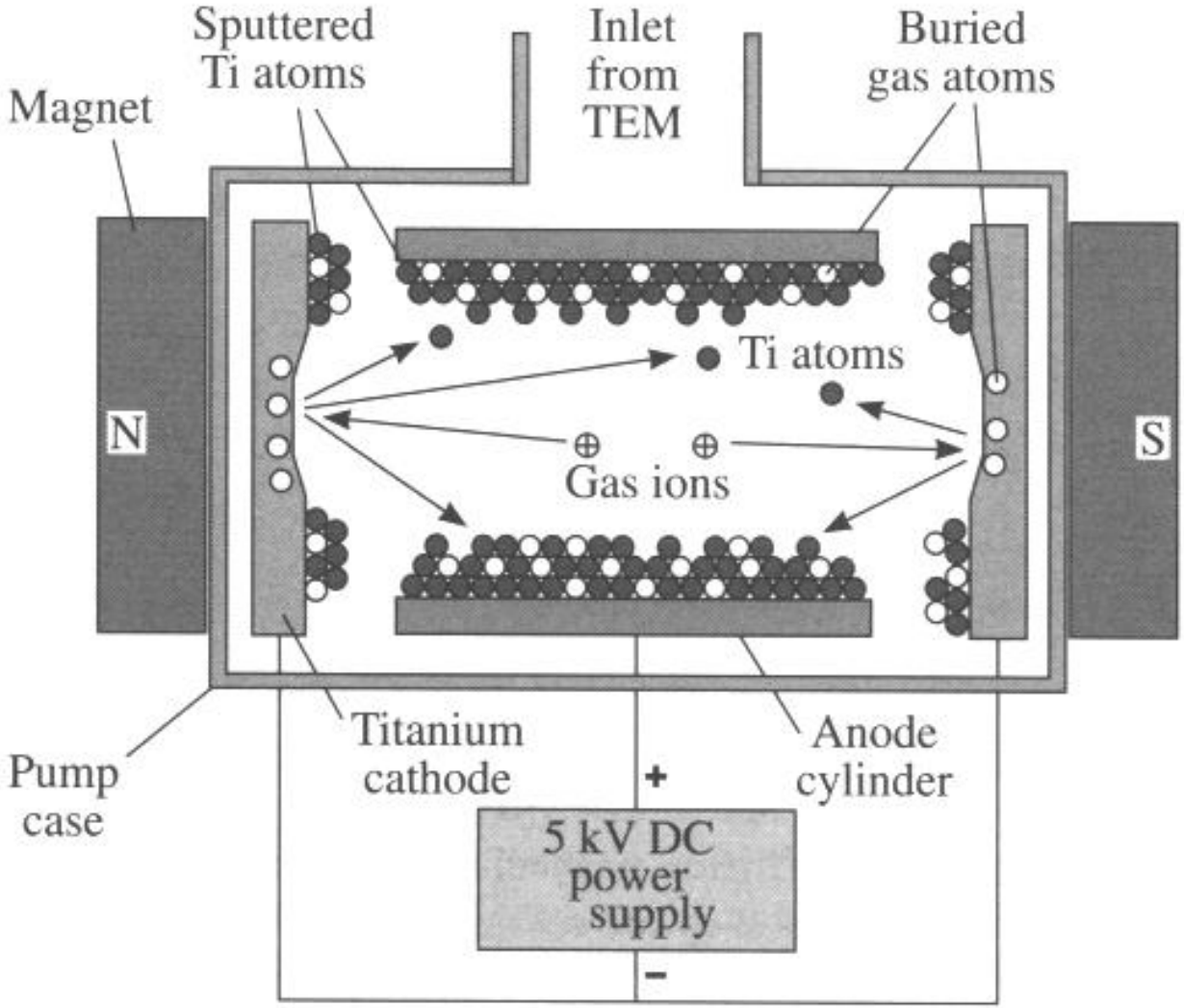

Figure 8.4. Schematic diagram showing how ion pumps trap ionized gas atoms by layers of Ti atoms at electrodes. Once trapped, the ions cannot escape until the pump is turned off.

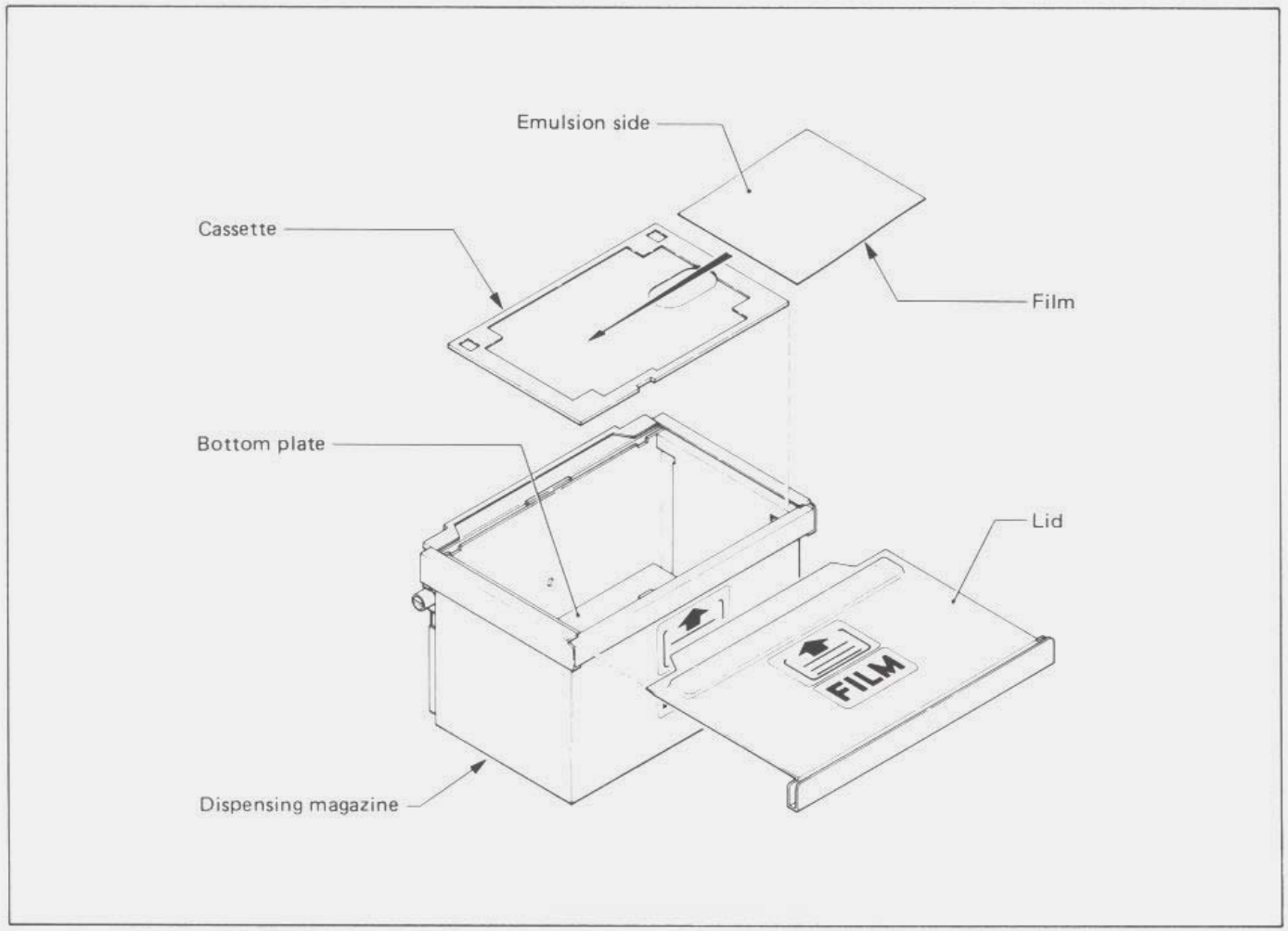

Fig. 5.2-1 Loading films into the dispensing magazine

5.2.2b Inserting (or removing) the magazines into (or from) the camera chamber

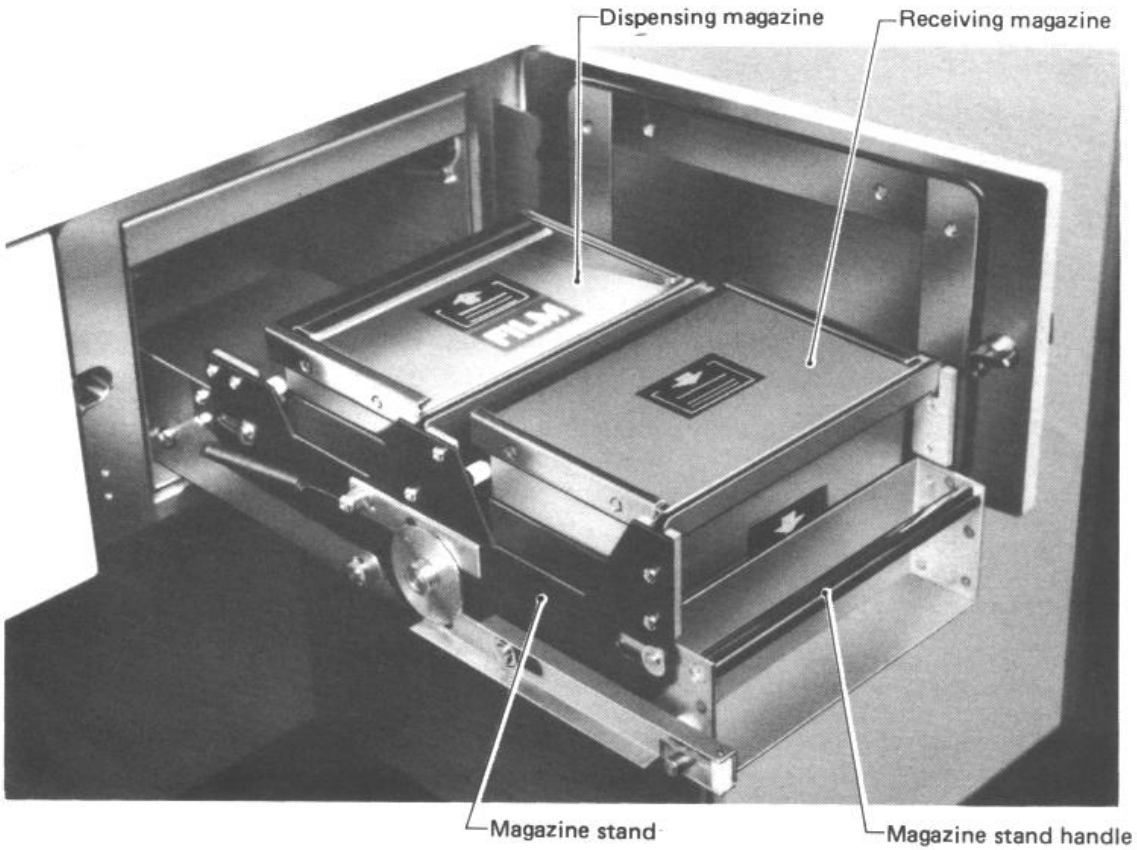

Fig. 5.2-5 Magazine stand

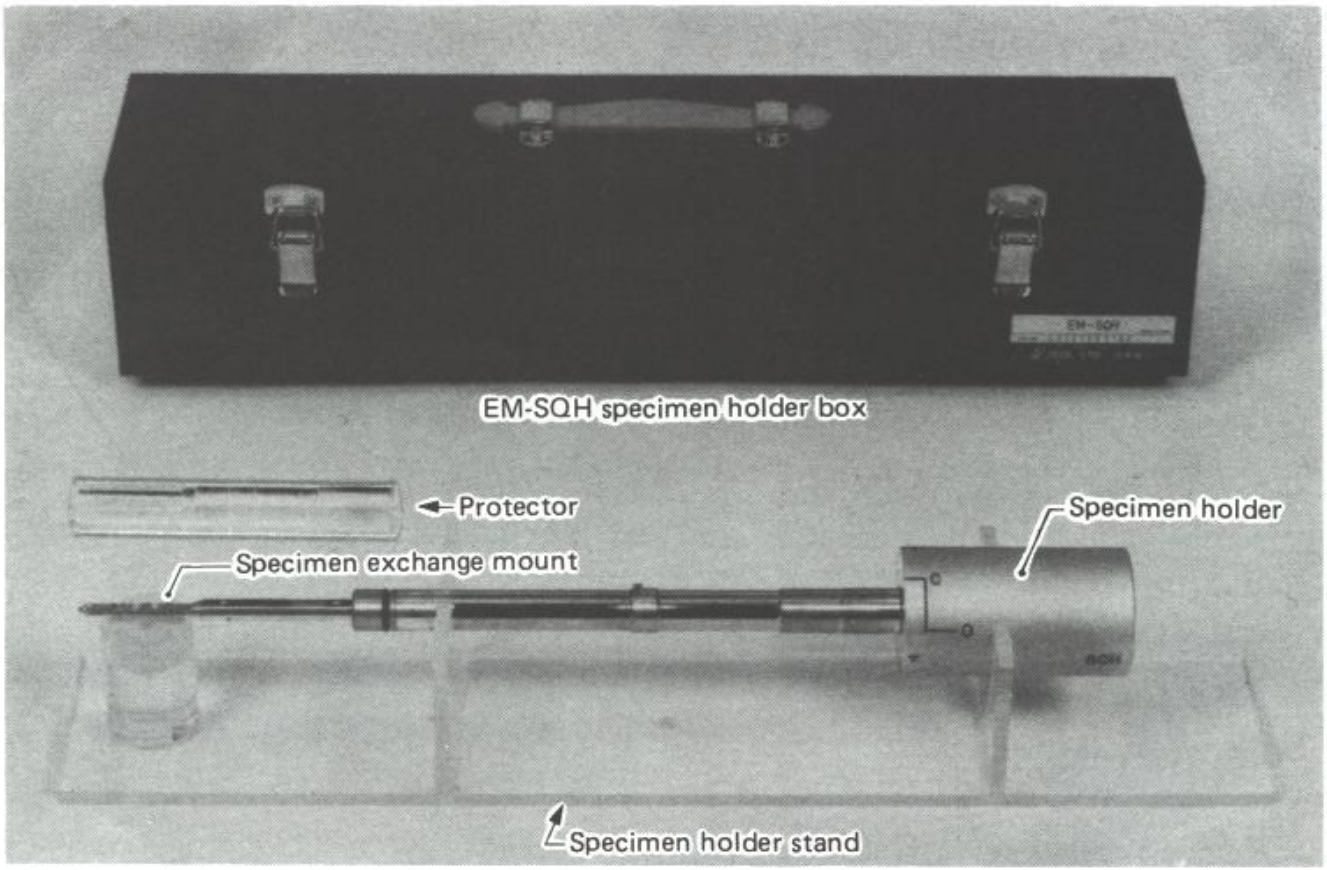

Fig. 5.2-7 EM-SQH specimen holder box and stand

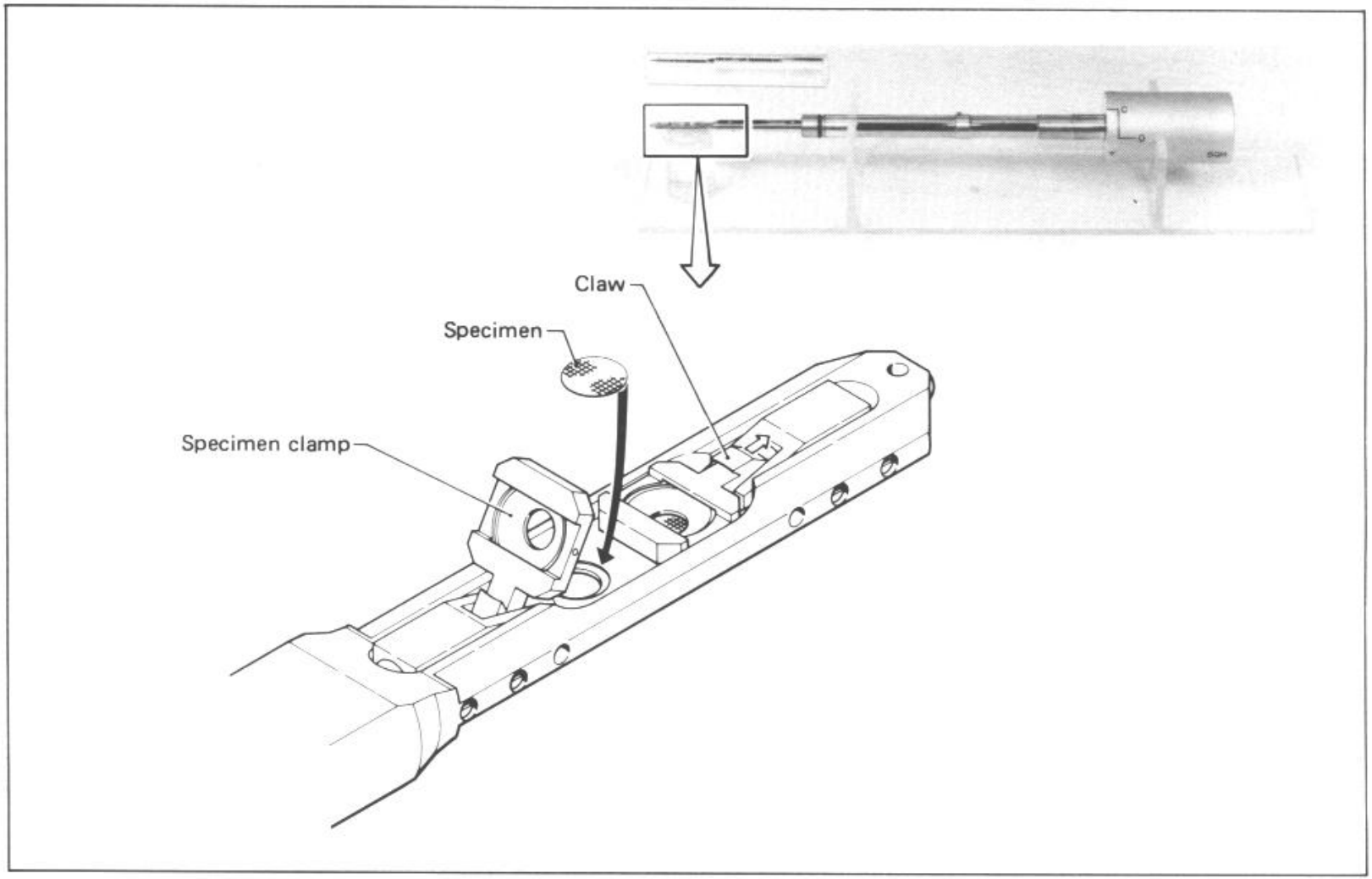

Fig. 5.2-9 Specimen exchange

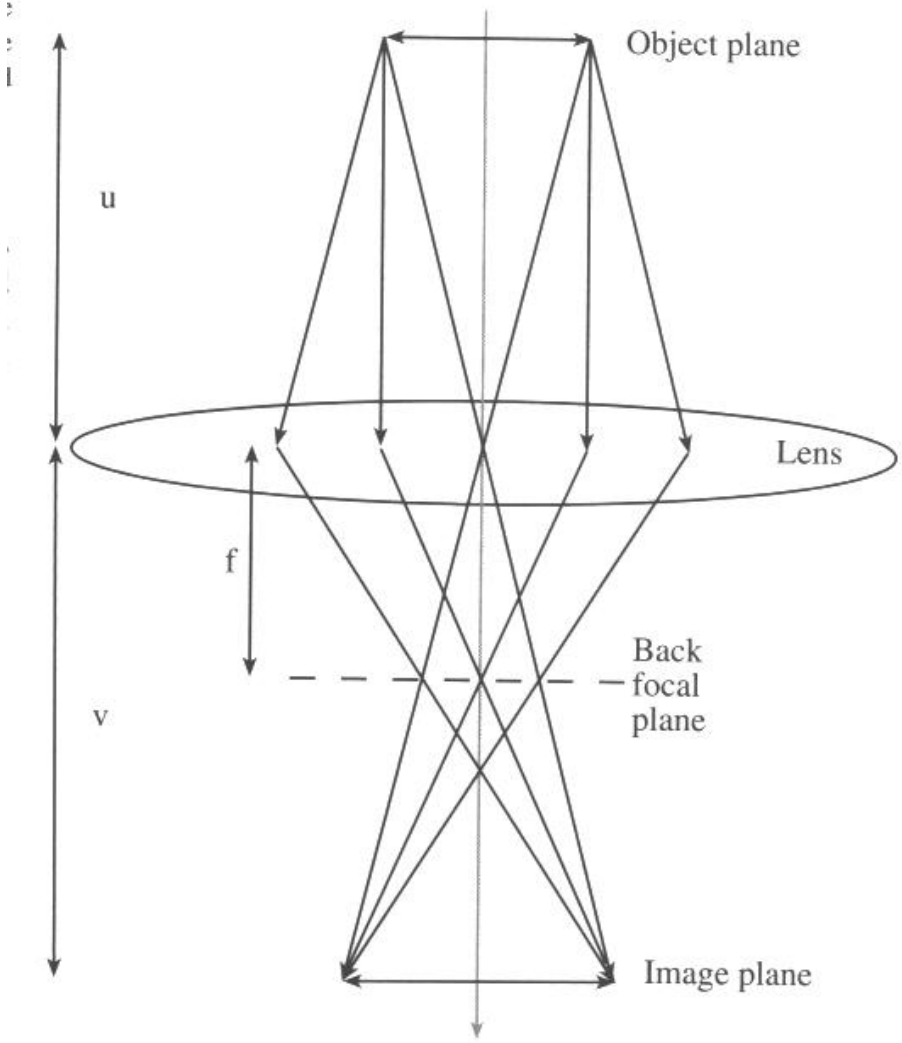

Figure 6.3. A complete ray diagram for a finite object, symmetrically positioned around the optic axis. All rays emerging from a point in the object (distance u from the lens) that are gathered by the lens converge to a point in the image (distance v from the lens) and all parallel rays are focused in the focal plane (distance f from the lens).

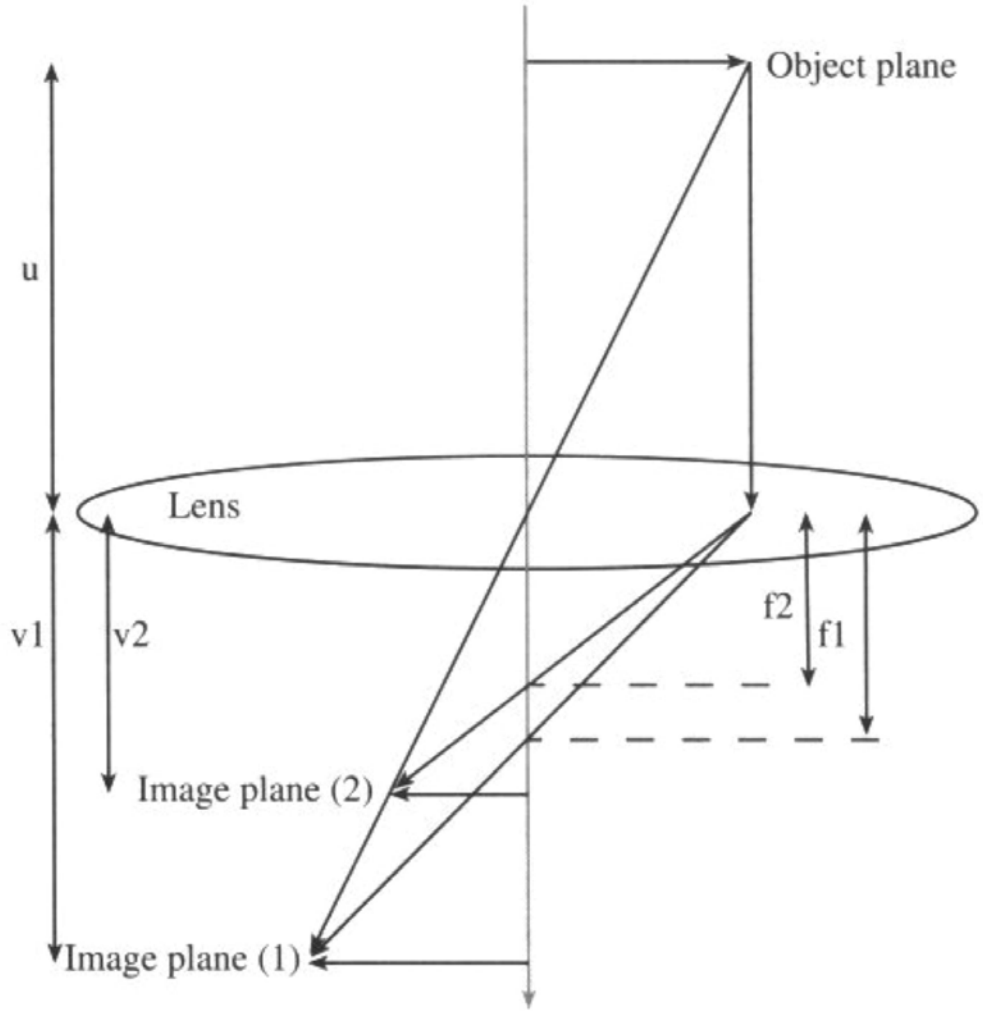

Figure 6.4. Strengthening the lens shortens the focal length f. So a weaker lens ($f1$) produces a higher magnification of the object than a stronger lens ($f2$) since the image distance v increases, but the object distance is unchanged.

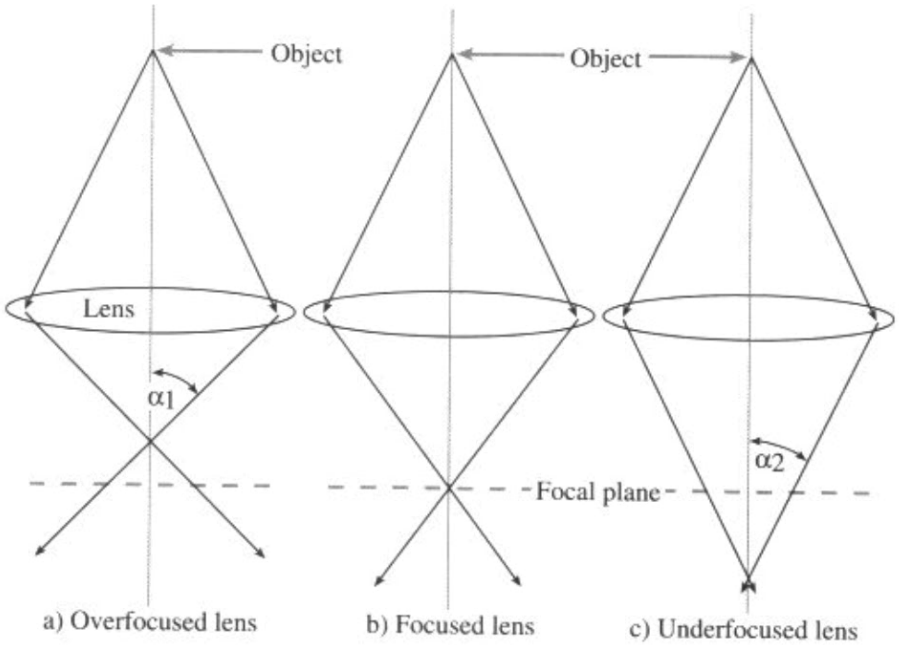

Figure 6.5. (a) Ray diagram illustrating the concepts of overfocus, in which a strong lens focuses the rays before the image plane, and (c) underfocus, where a weaker lens focuses after the image plane. It is clear from (c) that at a given underfocus the convergent rays are more parallel than the equivalent divergent rays at overfocus ($\alpha_2 < \alpha_1$).

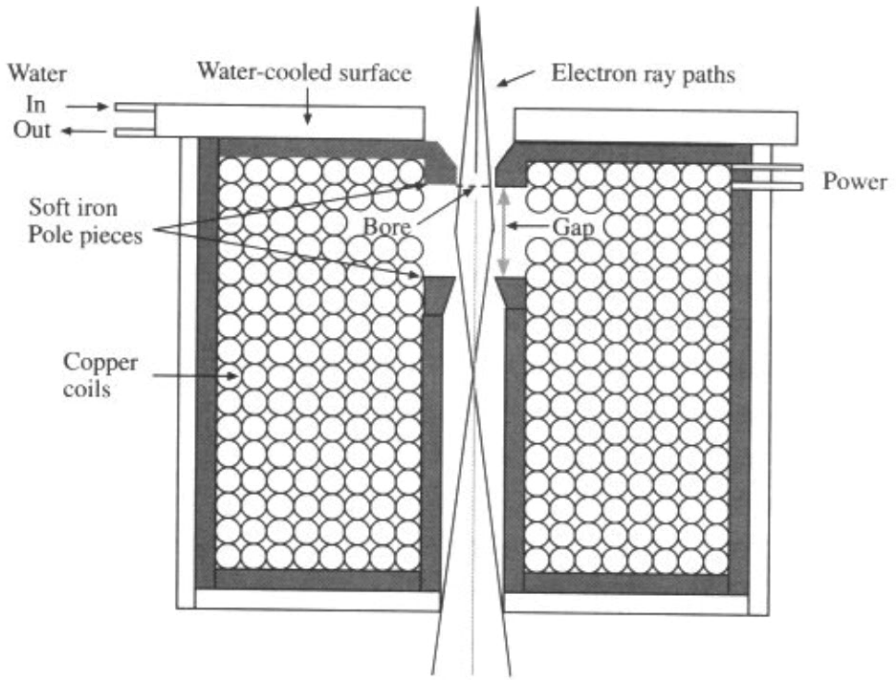

Figure 6.6. Schematic diagram of a magnetic lens. The pole pieces surround the coils and, when viewed in cross section, the bore and the gap between the polepieces are visible. The magnetic field is weakest on axis and increases in strength toward the side of the polepiece, so the electrons are more strongly deflected as they travel off axis.

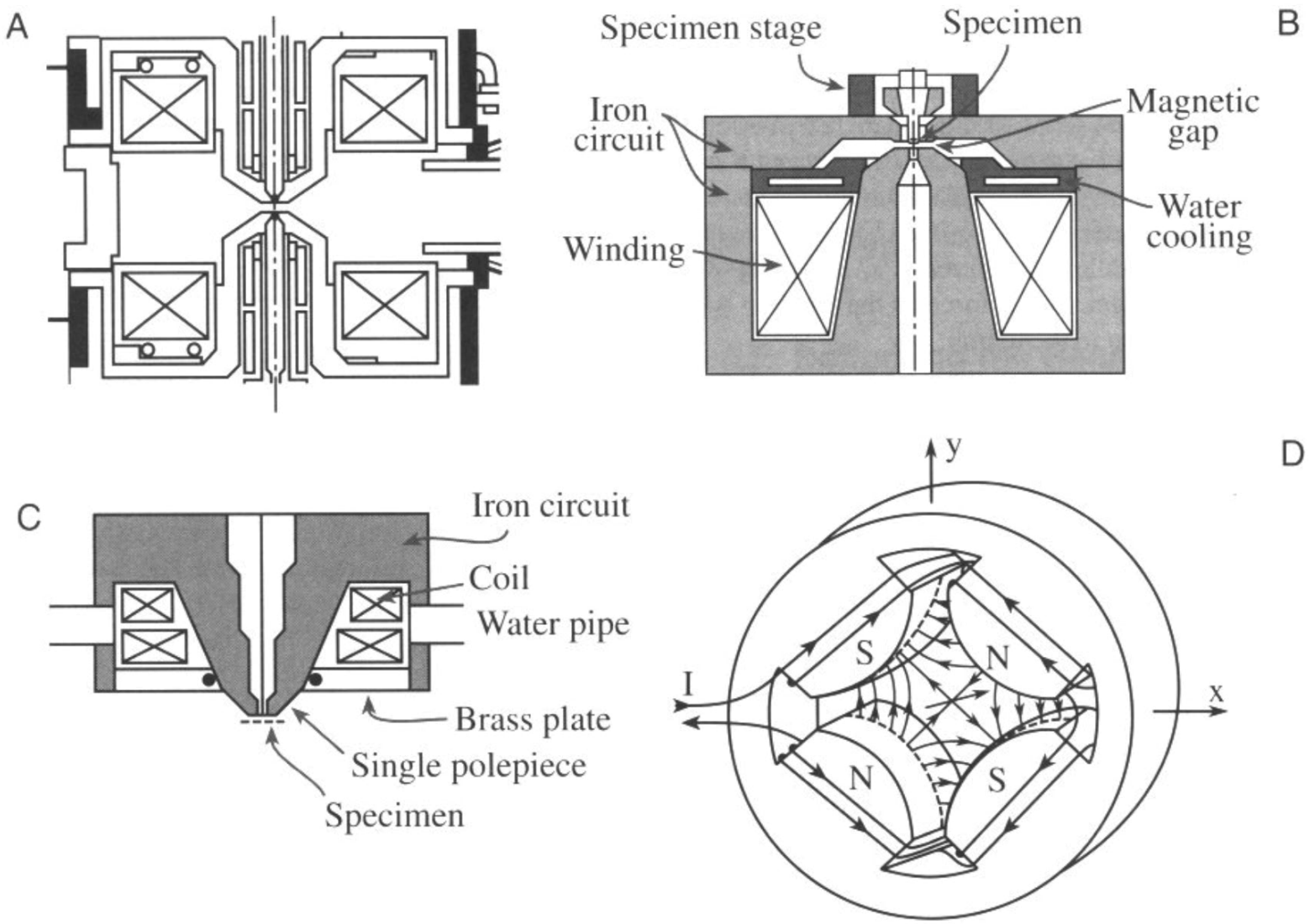

Figure 6.8. A selection of different lenses: (A) a split polepiece objective lens, (B) a top-entry immersion lens, (C) a snorkel lens, and (D) a quadrupole lens.